Effects of Molecular Weight of Polyvinylpyrrolidone on Precipitation Kinetics During the Formation of Asymmetric Polyacrylonitrile Membrane

JONG SEOK KANG, YOUNG MOO LEE

National Research Laboratory for Membranes, School of Chemical Engineering, College of Engineering, Hanyang University, Seungdong-ku, Seoul 133-791, South Korea

Received 2 January 2001; accepted 28 June 2001

ABSTRACT: The effects of the molecular weight of polyvinylpyrrolidone (PVP) on the precipitation kinetics during the formation of an asymmetric polyacrylonitrile membrane and the resulting membrane morphology were investigated. The precipitation kinetics of a polyacrylonitrile membrane was explored using the light-transmission method and optical microscopic observation, with an emphasis on the effective diffusion coefficient of the nonsolvent as a measure of the solvent/nonsolvent exchange rate. The retarded precipitation behaviors were not observed in all dope solutions. Also, the phase-separation rate was steeply decreased with the amount of PVP. It was deduced that increase of the viscosity of the polymer solution upon the addition of PVP hindered the intrusion of the nonsolvent, resulting in a decrease of the phase-separation rate. When the same amount of PVP with a different molecular weight was used, the precipitation rate decreased with increase of the molecular weight of PVP. Therefore, the nonsolvent tolerance, the interaction between PVP and H_2O, as well as the viscosity are regarded as important factors influencing the precipitation rate. The effective diffusion coefficient of the nonsolvent is closely related to the nonsolvent tolerance of the polymer solution, resulting from a pseudoternary phase diagram. The use of high molecular weight PVP strongly depressed the formation of macrovoids inside of the membrane and allowed a dense skin layer to form. © 2002 Wiley Periodicals, Inc. J Appl Polym Sci 85: 57–68, 2002

Key words: membranes; phase diagram; morphology

INTRODUCTION

Since the phase-inversion process was reported by Loeb and Sourirajan,[1] this method has become a standard technique to prepare asymmetric membranes. When a spread polymer solution film is in contact with a nonsolvent, the homogeneous polymer solution is separated into two phases: a polymer-rich phase and a polymer-lean phase, which is solidified and forms a rigid structure of the membrane and the pore, respectively. The final structure of such a membrane, which determines the transport characteristics of the resulting membrane, is greatly affected by the physical and chemical properties of the components such as the polymer, solvent, nonsolvent, and additives. The structure of an asymmetric membrane mainly observed is either a dense top layer sup-

Correspondence to: Y. M. Lee (ymlee@hanyang.ac.kr).
Contract grant sponsor: Korea Ministry of Science and Technology, National Research Laboratory Program.

Journal of Applied Polymer Science, Vol. 85, 57–68 (2002)

ported by a fine porous layer containing pores of similar sizes or a thin top layer supported by a very porous layer containing macrovoids.[2,3] The former is often called a sponge structure, and the latter, a fingerlike structure. However, the membrane structure with macrovoids, usually compared to that without macrovoids, has poor mechanical strength, so that such a membrane may not maintain its integrity under high operating pressure. Therefore, a membrane having a spongelike structure is still very much required for its application in the membrane process.

Extensive efforts, including the addition of organic or inorganic components as the third component to a dope polymer solution, have been devoted to yield recipes for preparing asymmetric membranes with desirable structures that suppress macrovoids and defects.[4–6] The addition of a polymer additive like poly(ethylene oxide) (PEG) and polyvinylpyrrolidone (PVP) to the polymer solution drastically changes the structure of the membrane. Particularly, PVP, in a dope solution, has been reported as a pore-forming agent, enhancing the permeation properties and suppressing the formation of macrovoids.[7]

There have been several attempts to explain the mechanism of membrane formation of the solution with PVP and its performance. Cabasso et al.[8] suggested that when microphase demixing between the two polymers took place the formation of the dense top layer was difficult. Roesink[9] found out that thin PVP walls between the pores, which broke upon drying the polyetherimide (PEI)/PVP membrane, caused the interconnectivity of the pores in the microfiltration membrane. The investigation of Boom et al.[2,3,7] on quaternary systems of polyethersulfone (PES)/PVP/1-methyl-2-pyrrolidinone (NMP)/H_2O showed that delayed demixing did not occur in such systems, due to separation between the polymer and the additive. They defined two time scales for diffusion: One is a short time scale for diffusion of the solvent and nonsolvent between PES and PVP, which is considered the first moments after immersion. Under this condition, two polymers are regarded as one constituent and this system can be treated as a pseudoternary system. It was found that when the additive content increased in the polymer solution the virtual system could contain much of the nonsolvent water without demixing, increasing the miscibility gap. On the other hand, there is a long time scale for the diffusion of the two polymers. When phase separation takes place slowly, the polymer and additive begin to separate.

The asymmetric structure of the membrane is controlled mainly by the kinetic effect, which is normally expressed as the exchange rate of the solvent and the nonsolvent.[10–12] The exchange rate depends upon the temperature, the viscosity of the solution,[13,14] and the nonsolvent tolerance of the polymer solution and so on. Also, the addition of a polymeric additive (PVP) into the polymer solution is a common way to alter the precipitation rate. Smolders et al.[2] concluded, from their calculations for predicting the membrane structure, that instantaneous liquid–liquid demixing led to a fingerlike structure with a thin top layer suitable for ultrafiltration and microfiltration membranes and the delayed demixing often yielded a sponge structure with a dense layer. Therefore, estimating the demixing behavior will help predict the membrane structure.

Until now, only a few commercial polymers such as polysulfone, PES, and PEI were investigated to determine the effects of the addition of PVP on the morphology and performance of a membrane. However, the effect of PVP on the formation of an asymmetric polyacrylonitrile (PAN) membrane has not been carried out so far. In this study, the precipitation kinetics and morphology during the formation of an asymmetric PAN membrane were studied upon varying the molecular weight of PVP in the solution of PAN/dimethylsulfoxide (DMSO) using a light-transmission apparatus and optical microscopy.

EXPERIMENTAL

Materials

Polymer solutions were prepared using PAN (Taekwang Ind.Co., Ltd.; M_n = 150,000) as a base polymer. DMSO (Aldrich Chemical Co., Milwaukee, WI) and first-distilled water were used as a good solvent and a precipitant, respectively. PVPs, purchased from Aldrich, were used as polymeric additives in a casting solution and their average molecular weights were 10, 55 and 1300 kDa, respectively. PAN and PVP were dried under a vacuum at 60°C for 2 h to minimize the presence of water in the polymer prior to the preparation of the solution. DMSO was used as received without further purification.

Table I Composition of Polymer Solution for the Preparation of Membrane

Sample Code	PVP (MW, wt %)	PAN (wt %)	DMSO (wt %)
N	—	8	92
A1	10 K, 1	8	91
A3	10 K, 3		89
A5	10 K, 5		87
A8	10 K, 8		84
B1	55 K, 1	8	91
B3	55 K, 3		89
B5	55 K, 5		87
B8	55 K, 8		84
C1	1300 K, 1	8	91
C3	1300 K, 3		89
C5	1300 K, 5		87
C8	1300 K, 8		84

Preparation and Characterization of PAN Membrane

Asymmetric flat membranes were prepared by the wet phase inversion technique. PAN and PVP were used as a membrane-forming polymer and pore-forming agent, respectively. Polymer dope solutions were prepared by increasing the concentration or the molecular weight of PVP while the total concentration of PAN in the solution was maintained at 8 wt %. The compositions of the polymer solution are presented in Table I.

The casting solution was spread onto a glass plate with a 250-μm casting knife and immersed immediately into a water bath at 27°C, wherein it is important that the temperature of the water must be beyond the melting point of DMSO of 18.4°C. Cast film was preserved in the water bath for 24 h and then dried for 2 days in the air. Cross-sectional morphologies of the membranes were taken using scanning electron microscopy (SEM; Hitachi S–510, Japan).

For measuring the oxygen permeance, a membrane of 2 cm in diameter was placed in a conventional gas permeation cell as shown in Figure 1. The oxygen flux at the steady state was measured with a flowmeter (Varian Analytical Instruments, USA), from which the oxygen permeance (P) was calculated from the following equation:

$$P = \frac{\Delta Q}{A \Delta t \Delta P} \quad (1)$$

where ΔQ (cm^3) is the quantity of gas at STP that permeates during the time interval Δt (s) in a steady-state flow; A (cm^2), the effective membrane area; and ΔP (cmHg), the pressure difference. GPU denotes the gas permeation unit:

$$1 \text{ GPU} = 10^{-6} \frac{\text{cm}^3 \text{ (STP)}}{\text{cm}^2 \text{ s cmHg}}$$

Pseudoternary Phase Diagram

In many membrane-forming systems, two polymers can be regarded as one polymer.[7,12,15] Of course, this simplification is accompanied by the restriction of homogeneity between two polymers, namely, on the assumption that during the first moments after immersion two polymers do not relatively separate from each other; the two polymers are considered as one polymeric network and the system can be treated as pseudoternary. Therefore, it is convenient to lump two polymers (PAN, PVP) together to investigate the effect of the molecular weight of PVP on the variation of the binodal line in the pseudoternary phase diagram. The ratio of the weight percentage of two polymer components was fixed to 1 ($\phi_{PAN}/\phi_{PVP} = 1$) as shown in Table II. The separation between the polymer-rich phase and the polymer-poor phase in the pseudoternary system was determined from the turbidity measurement.

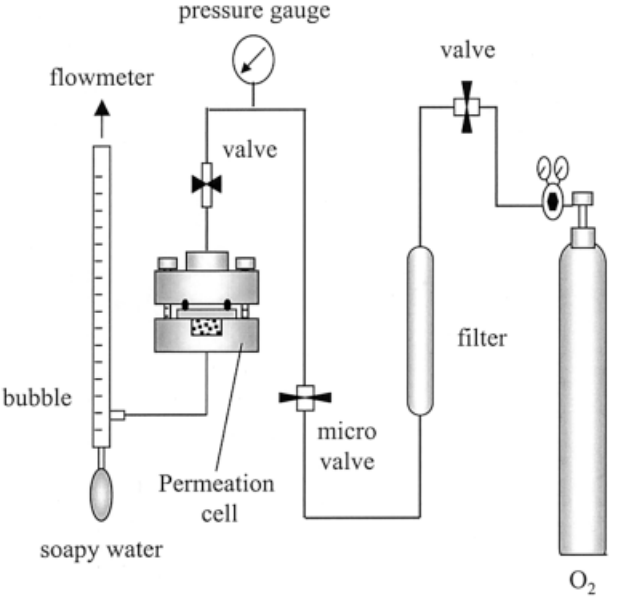

Figure 1 Schematic of gas permeance cell apparatus.

Table II Composition of Polymer Solution Investigated for Turbidity Measurement

PAN (wt %)	PVP (MW, wt %)	H_2O (wt %)	DMSO (wt %)	Turbidity
7	10 K, 7	6	80	C
5	10 K, 5	6	84	C
2	10 K, 2	6	90	C
1	10 K, 1	8	90	C
5	10 K, 5	8	82	T
2	10 K, 2	8	88	T
1	10 K, 1	10	88	T
5	55 K, 5	7	83	C
2	55 K, 2	7	89	C
1	55 K, 1	9	89	C
5	10 K, 5	9	81	C
2	55 K, 2	9	87	T
1	55 K, 1	11	87	T
5	1300 K, 5	10	80	C
4	1300 K, 4	10	82	C
2	1300 K, 2	10	86	C
1	1300 K, 1	12	86	C
4	1300 K, 4	12	80	T
2	1300 K, 2	12	84	T
1	1300 K, 1	14	84	T

C: clear; T: turbid.

The cloud points or turbidities were determined by a simple titration measurement. A test tube filled with a dope solution composed of PAN/PVP/DMSO was placed in an isothermal bath at 27°C. With a syringe, first-distilled water was very slowly added to the solution until the initially clear solution became visually turbid.[16] The pseudoternary phase diagram was obtained from the cloud points.

Light-transmission Experiment

A halogen lamp used as the light source was positioned at a distance of 25 cm from the dope solution. An incident light was directly exposed on the surface of a cast dope solution, a part of the contact with the precipitant, and then the transmitted light intensity was detected from the bottom of the cast dope solution, a part of the contact with the glass plate, by a photodiode. This signal was synchronously accepted through an A/D converting treatment. A cast solution film was immersed in a precipitant (H_2O) and the intensity of the transmitted light through the dope solution during phase separation was measured as a function of time. The intensity of the transmitted light decreased with the progress of phase separation. The discrimination between instantaneous demixing and delayed demixing can be readily ob-

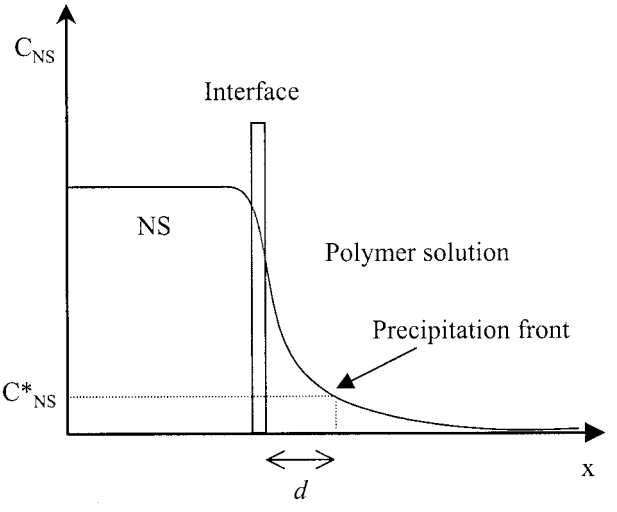

Figure 2 Schematic illustration of the concentration profile of nonsolvent C_{NS} during the immersion precipitation. C^*_{NS} and d are the nonsolvent concentration and the precipitation distance of the precipitation front, respectively.

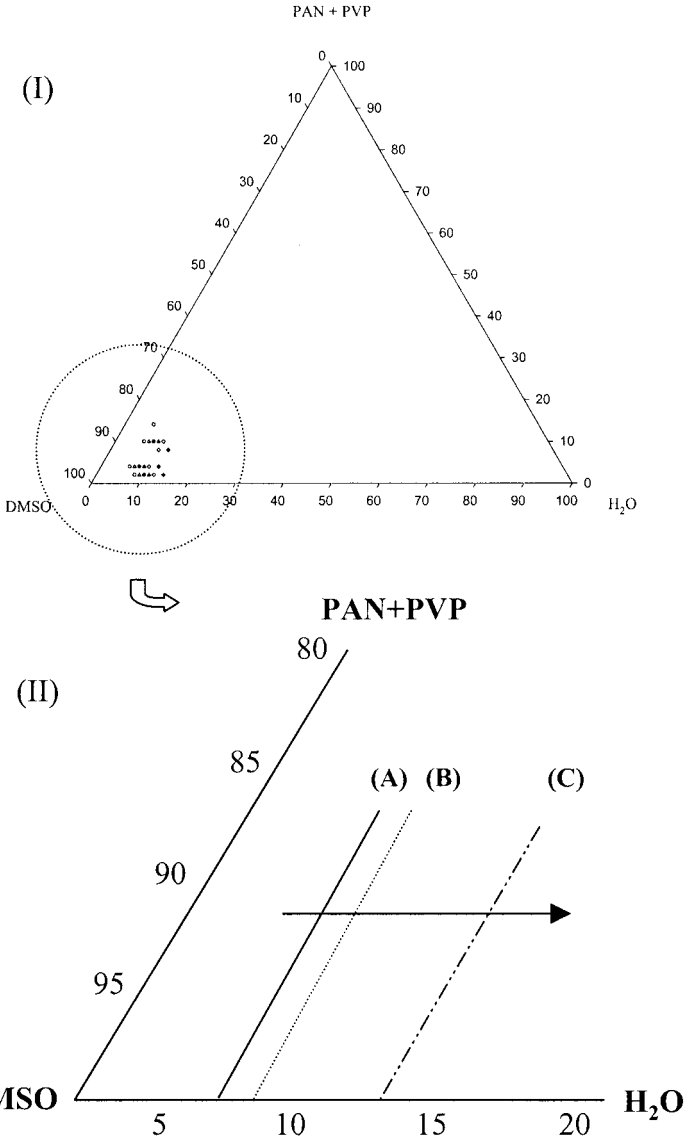

Figure 3 Pseudoternary phase diagram of polymer solution: (I) real plot of Table II; (II) enlarged schematics of the dotted circle of (I). (A) PVP MW 10 kDa [(○) C; (●) T]; (B) PVP MW 55 kDa [(△) C; (▲) T]; (C) PVP MW 1300 kDa [(◇) C; (◆) T].

served. The demixing rate can be detected upon varying the molecular weight or the amount of PVP.[17] An apparatus for the light transmission can be found in refs. 3, 7, 16, and 18.

Optical Microscope Observation

After placing a drop of the polymer solution between two optical slide glasses, a drop of H_2O was introduced near the edge of the spread polymer solution with a syringe.[16] As H_2O, used as a precipitant, contacts with the polymer solution and subsequently diffuses into the polymer solution, precipitation starts to take place and its front moves inward. Since the nonsolvent penetration has already proceeded before precipitation starts, the measured point is not a penetration front of a nonsolvent but a precipitation front as schematically illustrated in Figure 2. The progressing distance, d, of the precipitation front was measured by an optical microscope (Nikon, Model Fax, Japan) taken at different time intervals. From this observation, the apparent diffusion coefficient of a nonsolvent can be calculated.

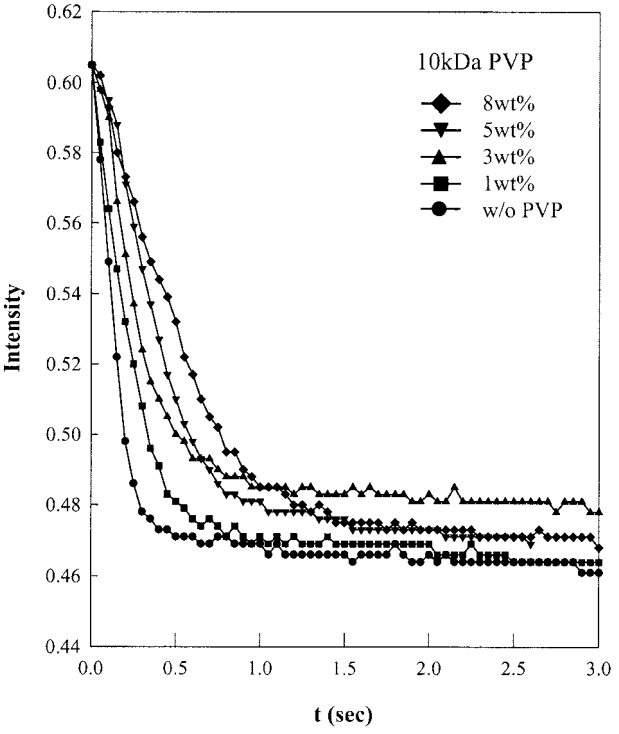

Figure 4 Effect of PVP (MW 10 kDa) on liquid–liquid demixing behavior.

RESULTS AND DISCUSSION

Pseudoternary Phase Diagram

The miscibility of the quaternary system was investigated and their virtual binodal lines of a pseudoternary phase diagram determined by turbidity are shown in Figure 3. (A), (B), and (C) denote 10, 55, and 1300 kDa PVP, respectively. This diagram was obtained from the cloud points and illustrates that the virtual binodal line shifted to the right with increase of the molecular weight of PVP. Consequently, the nonsolvent tolerance of the polymer solution increased. In other words, the solution containing 1300 kDa PVP has the highest nonsolvent tolerance and that of 10 kDa PVP has the lowest. When the nonsolvent tolerance is small, a small concentration fluctuation, for example, introduction of a small amount of a nonsolvent into the polymer solution, causes the polymer solution to be readily separated into two phases. Therefore, it was deduced that increase of the nonsolvent tolerance with the molecular weight of PVP caused the slowing of the precipitation rate.

Precipitation Kinetics During PAN Membrane Formation

In this study, under the thermodynamically more unstable casting condition produced by increasing the molecular weight or the concentration of PVP, the delayed demixing behaviors were not observed in all dope solutions, as shown in Figures 4–6. This result was in accordance with the previous findings by Boom et al.,[3] Borges et al.,[10] and McHugh et al.[11] Although increase of the absolute viscosity of the dope solution after the addition of PVP would result in a decrease of the exchange rate between the solvent and nonsolvent during phase separation, the instantaneous demixing observed in PVP-containing solutions was due to the strong mutual affinity between DMSO and H_2O, rather than between NMP and H_2O. This was supported by the fact that the mutual diffusion coefficient of DMSO/H_2O was 10×10^{-6} cm^2/s, while that of NMP/H_2O was 5.45×10^{-6} cm^2/s at a partial weight fraction of 0.5.[19,20] In addition, it was important that the interaction between PVP and H_2O was very strong.

We could plot a linear equation from one point ($t = 0$) to several initial points. From this linear

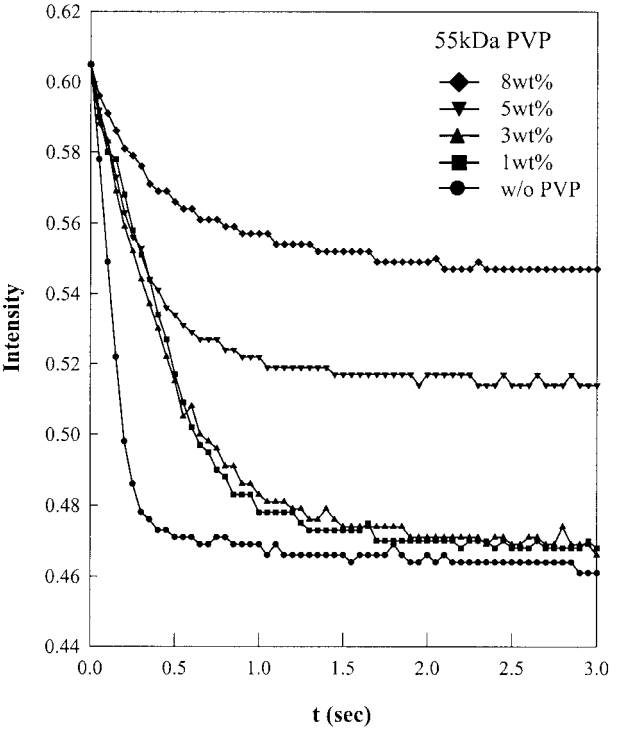

Figure 5 Effect of PVP (MW 55 Da) on liquid–liquid demixing behavior.

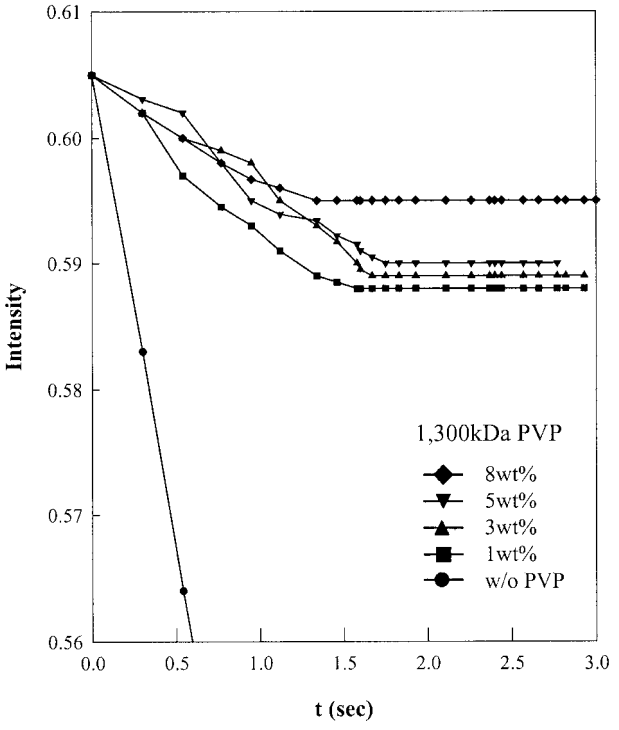

Figure 6 Effect of PVP (MW 1300 kDa) on liquid–liquid demixing behavior.

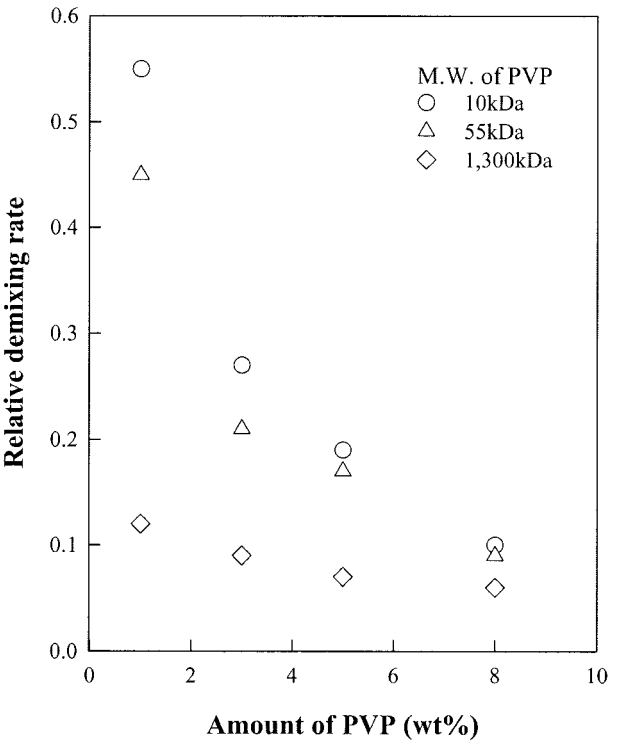

Figure 7 Effect of molecular weight of PVP as additive used on demixing rate.

equation, we obtained the absolute value of the slope. The absolute values from the initial slope of each curve presented in Figures 4–6 are plotted in Figure 7. This figure illustrates the effect of the PVP used as an additive on the precipitation rate. For PVP having the same molecular weight, the phase-separation rate steeply decreased with the amount of PVP. The influence of PVP with a relatively low molecular weight (10 and 55 kDa) on the precipitation rate was regarded as very strong, while that of the high molecular weight (1300 kDa) was weak. It is reasonable to assume that the increasing viscosity of the dope solution with the amount of PVP caused the slowing of the precipitation rate.

The exchange rate of a solvent and a nonsolvent at the interface between the polymer solution and the nonsolvent played an important role in controlling the membrane morphology and performance.[21–23] For the measurement of the precipitation rate of the nonsolvent, optical microscopy was used in this study. The nonsolvent precipitation rate was investigated by measuring the traveling distance of the precipitation front as a function of time. Figure 8 schematically illustrates the simplified membrane-formation procedure as the nonsolvent penetrates into the polymer solution.

Figure 9 shows optical micrographs (×100) taken as a function of time, where the dark area presents the precipitated area. As can be seen in this figure, the precipitation rate for the solution with 10 kDa PVP (A8) is much faster than that for the solution with 1300 kDa PVP (C8). The precipitation distance (d) of the precipitated front was taken with the time (t) and plotted with the square root of the time as presented in Figure 10. As the penetration distance is linearly proportional to the square root of the time, it was clear that the diffusion of the nonsolvent complied with Fickian behavior. The approach to obtain the ef-

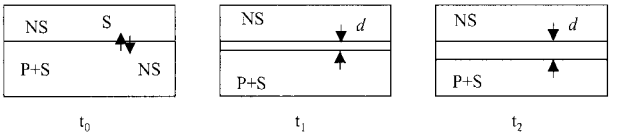

Figure 8 Schematics of membrane formation with time.

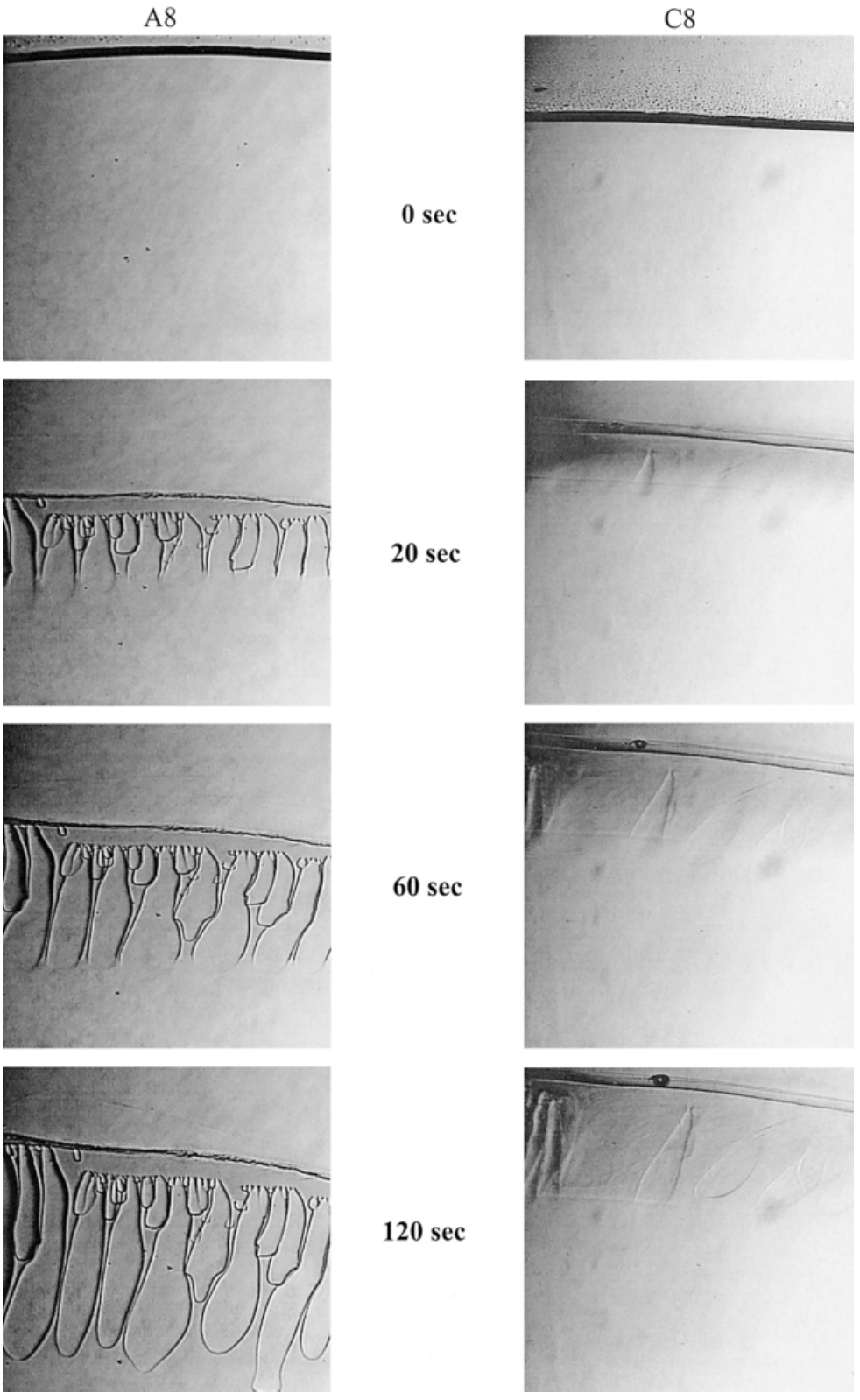

Figure 9 Optical micrographs for H_2O penetration taken with time through the polymer solutions A8 and C8. The number denotes the elapsed time (s).

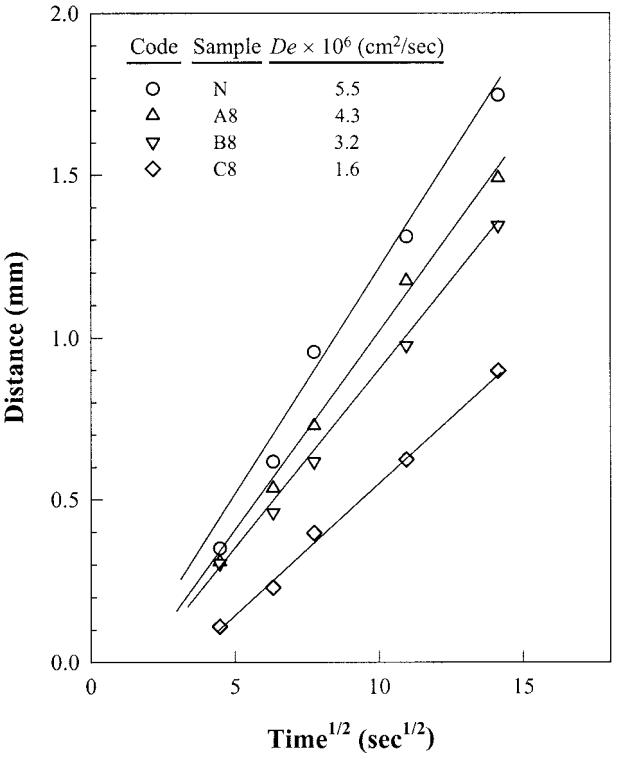

Figure 10 Plot of the penetration distance (d) of precipitation for a solution.

fective diffusion coefficient of the penetrant can be represented by the following equation:

$$d = 2(D_e t)^{1/2} \quad (2)$$

where D_e is the effective diffusion coefficient of the nonsolvent. The calculated D_e values are shown in the legend in Figure 10. D_e decreased with increase of the molecular weight of PVP in the polymer solution. This implies that the nonsolvent tolerance is closely related to the diffusion coefficient of the nonsolvent. In other words, a low nonsolvent tolerance of the polymer solution corresponds to a higher diffusion coefficient of the nonsolvent and a high nonsolvent tolerance of the polymer solution corresponds to a lower diffusion coefficient. Accordingly, for the same amount of PVP, the decrease of the precipitation rate upon the increase of the molecular weight of PVP could be understood from the increment of nonsolvent tolerance and the viscosity of the polymer solution.

Morphology and Oxygen Permeation of Membranes

The cross-sectional morphologies of typical membranes prepared as in Table I were observed by SEM. Typical pictures are shown in Figure 11(A,B). It was observed that the membrane morphology strongly depended on the amount as well as on the molecular weight of PVP. The cross-sectional morphologies of the membrane prepared with 10 kDa PVP (A1–A8) and 55 kDa PVP (B1–B8) showed macrovoids and the thickness of the spongelike structure slightly increased. However, membranes prepared with 1300 kDa PVP (C1–C8) showed that the sponge structure and macrovoids suddenly disappeared at >5 wt % PVP content. The representative SEM photographs of the cross section of the N, A8, B8, and C series membranes are shown in Figure 11(A). SEM photographs of the skin layer of the membrane (×5000) are also presented in Figure 11(B). From these SEM micrographs, the effect of the molecular weight of PVP on the variation of the spongelike structure was elaborated by the percentage of the length from the skin to the initially formed macrovoids divided by the membrane thickness, as presented in Figure 12. The percentage of the spongelike structure (%) could be simply defined as a one-dimensional effect of PVP on the promotion of the spongelike structure in the cross sections of the membrane finally prepared. This result is in accordance with the precipitation behavior from optical microscopic observation as shown in Figure 9. Therefore, the use of high molecular weight PVP in the preparation of a PAN asymmetric membrane strongly depressed the formation of macrovoids.

To verify the dense property for the skin layer of the PAN membrane formed, their oxygen permeation properties were investigated using a gas permeation cell as mentioned in the Experimental section. The effect of the addition of PVP on the oxygen permeation is presented in Figure 13. As the molecular weight of PVP increased, the oxygen permeation decreased. Although the precipitation kinetics could not directly provide information on the formation of a skin layer and cross-sectional morphology, it was understood from the oxygen permeation test that this behavior of low oxygen permeation of the present membrane might be attributed to the dense skin layer

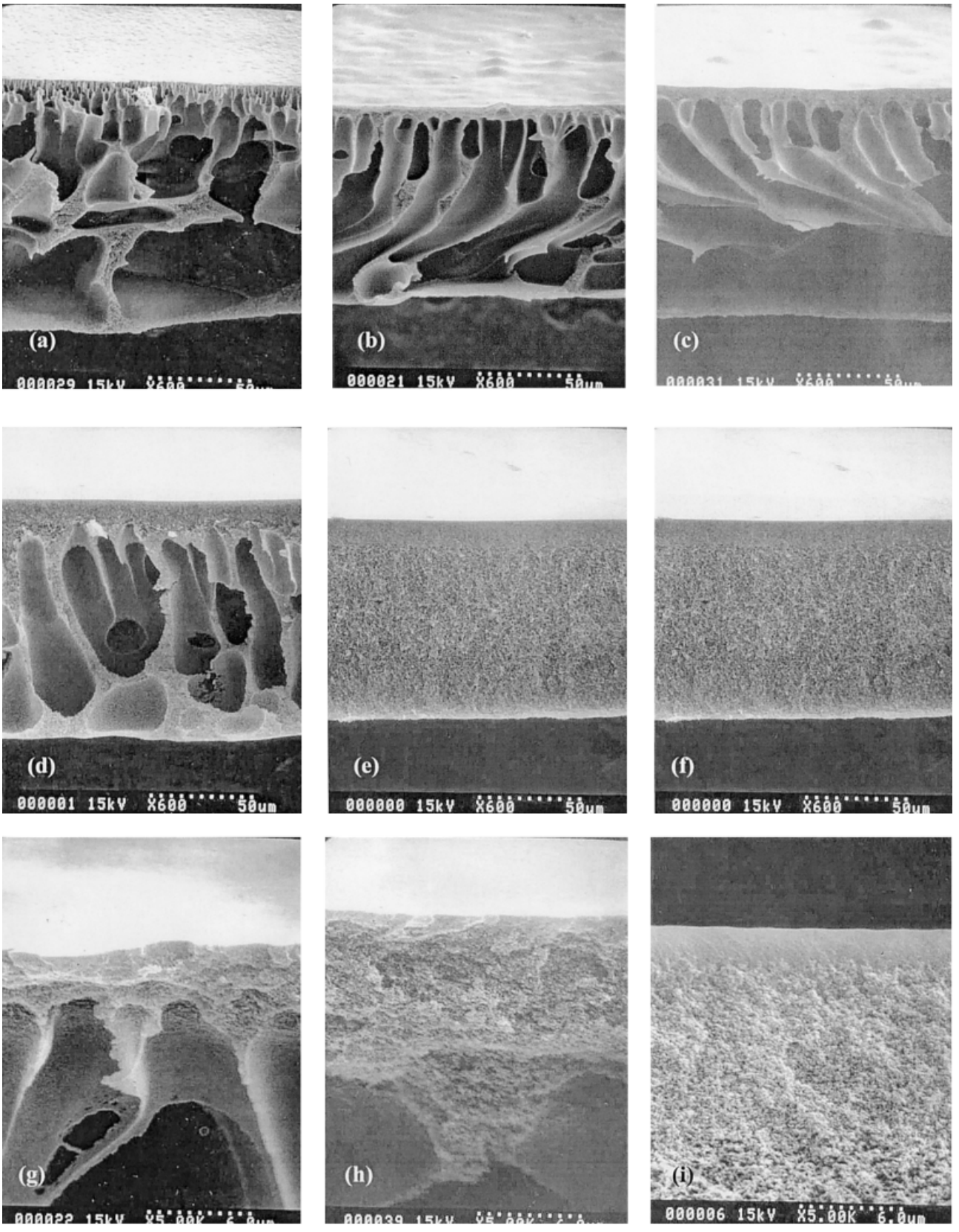

Figure 11 (A) SEM photographs of the cross section of the membranes: (a) N; (b) A8; (c) B8; (d) C8. (B) SEM photographs of the skin layer of the membranes enlarged with ×5000 magnification: (e) A8; (f) B8; (g) C8.

due to a slower precipitation rate with increase of the molecular weight of PVP.

CONCLUSIONS

In the immersion precipitation process for preparing asymmetric PAN membranes, the effects of the molecular weight of PVP used as an additive on the precipitation kinetics and membrane morphology were investigated. As the molecular weight of PVP in the polymer solution increased, the nonsolvent tolerance increased. Also, it was found that a polymer solution of low nonsolvent tolerance corresponded to a high diffusion coefficient of the nonsolvent and vice versa. Therefore, increase of the nonsolvent tolerance of a polymer solution upon the addition of high molecular weight PVP blocked the intrusion of a nonsolvent into the polymer solution, resulting in a decrease of the phase-separation rate. The cross-sectional morphology of a membrane prepared with high molecular weight PVP (1300 kDa) showed a spongelike structure without macrovoids. Consequently, the use of high molecular weight PVP in the preparation of a PAN asymmetric membrane had a strong effect on the depression of the formation of macrovoids. Particularly, macrovoids completely disappeared at >5 wt% PVP content. Moreover, from the oxygen permeation test, it was found that a denser skin layer for an asymmetric PAN membrane could be formed using of high molecular weight PVP.

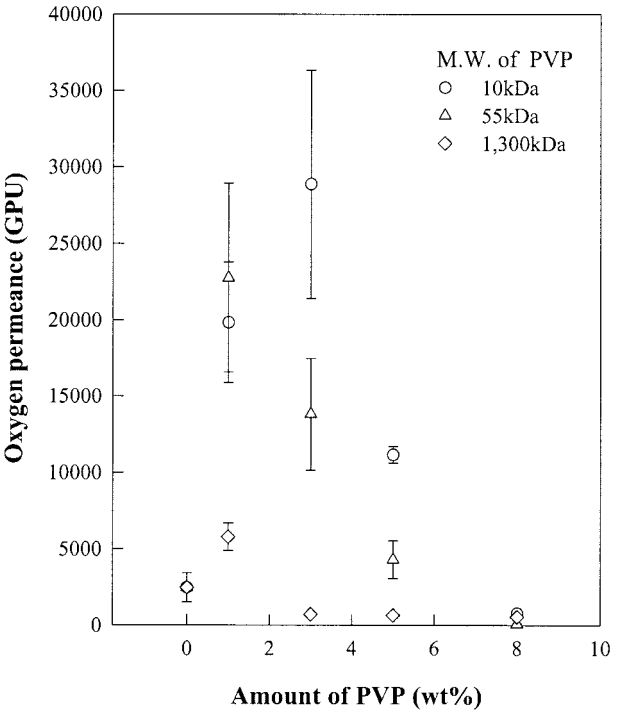

Figure 13 Effect of addition of PVP on the oxygen permeance. 1 GPU [gas permeation unit]: 10^{-6} cm^3 (STP)/cm^2 cmHg s.

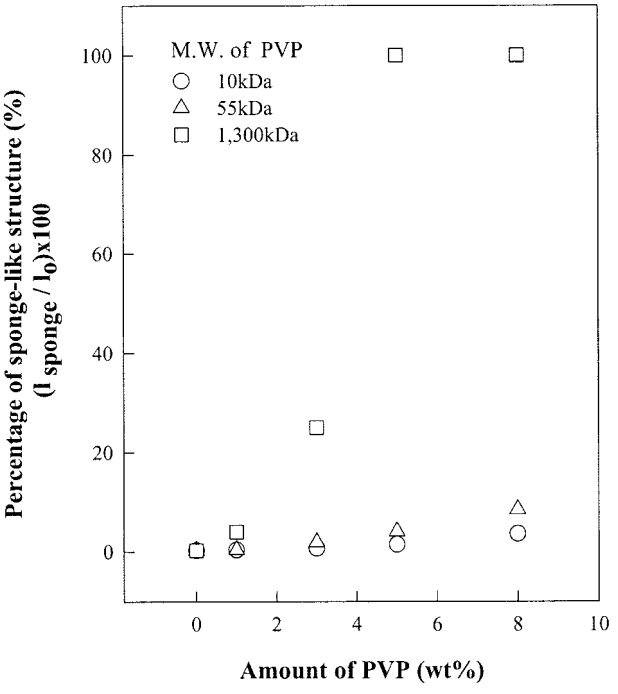

Figure 12 Effect of the molecular weight of PVP on the structure of the membrane: *y*-axis shows the percentage of the length from the skin to the initially formed macrovoids divided by the membrane thickness.

One of the authors (J. S. K.) is grateful to the Institute of Hanyang Brain Korea 21 for a scholarship. This work was supported by the Korea Ministry of Science and Technology under the National Research Laboratory Program in the year 2000.

REFERENCES

1. Loeb, S.; Sourirajan, S. Adv Chem Ser 1962, 38, 117.
2. Smolders, C. A.; Reuvers, A. J.; Boom, R. M.; Wienk, I. M. J Membr Sci 1992, 73, 259.

3. Boom, R. M.; van den Boomgaard, Th.; Smolders, C. A. J Membr Sci 1994, 90, 231.
4. Pinnau, I.; Koros, W. J. J Membr Sci 1992, 71, 81.
5. Lai, J. Y.; Lin, F. C.; Wang, C. C.; Wang, D. M. J Membr Sci 1996, 118, 49.
6. Perez, S.; Merten, E.; Robert, E.; Cohen Addal, J. P.; Viallant, A. J Appl Polym Sci 1993, 47, 1621.
7. Boom, R. M. Ph.D. Dissertation, The University of Twente, Enschede, The Netherlands, 1992.
8. Cabasso, I.; Klein, E.; Smith, J. K. J Appl Polym Sci 1977, 21, 165.
9. Roesink, H. D. W. Ph.D. Dissertation, University of Twente, The Netherlands, 1989.
10. Machado, P. S. T.; Habert, A. C.; Borges, C. P. J Membr Sci 1999, 155, 171.
11. Barton, B. F.; Reeve, J. L; McHugh, A. J. J Appl Polym Sci Part B Polym Phys 1997, 35, 569.
12. Graham, P. D.; Brodbeck, K. J.; McHugh, A. J. J Control Rel 1999, 58, 233.
13. Chung, T. S.; Hu, X. J Appl Polym Sci 1997, 66, 1067.
14. Chung, T. S.; Teoh, S. K.; Hu, X. J Membr Sci 1997, 133, 161.
15. Wienk, I. M; Boom, R. M; Beerlage, M. A. M.; Bulte, A. M. A.; Smolders, C. A.; Strathman, H. J Membr Sci 1996, 113, 361.
16. Wijmans, J. G.; Kant, J.; Mulder, M. H. V.; Smolders, C. A. Polymer 1985, 26, 1539.
17. Reuver, A. J. Ph.D. Thesis, Twente University of Technology, The Netherlands, 1987.
18. Cohen, C.; Tanny, G. B.; Prager, S. J Polym Sci Polym Phys 1979, 17, 477.
19. Tkacik, G.; Zeman, L. J Membr Sci 1987, 31, 273.
20. Barton, B. F. M.S. Dissertation, University of Illinois, Urbana, IL, 1996.
21. Wijmans, J. G.; Baaij, J. P. B.; Smolders, C. A. J Membr Sci 1983, 14, 263.
22. Wijmans, J. G.; Kant, J.; Mulder, M. H. V.; Smolders, C. A. Polymer 1985, 26, 1539.
23. Kang, Y. S.; Kim, H. J.; Kim, U. Y. J Membr Sci 1991, 60, 219.